Journal of Medicinal Chemistry

Article

pubs.acs.org/jmc

Novel Combretastatin-2-aminoimidazole Analogues as Potent Tubulin Assembly Inhibitors: Exploration of Unique Pharmacophoric Impact of Bridging Skeleton and Aryl Moiety

Vikas Chaudhary,[†,∥] Jubina B. Venghateri,[‡,∥] Hemendra P. S. Dhaked,[§] Anil S. Bhoyar,[†] Sankar K. Guchhait,[*,†] and Dulal Panda[*,§]

[†]Department of Medicinal Chemistry, National Institute of Pharmaceutical Education and Research (NIPER), Sector 67, SAS Nagar, Mohali, Punjab 160062, India

[‡]IITB-Monash Research Academy, Indian Institute of Technology Bombay, Mumbai 400076, India

[§]Department of Biosciences and Bioengineering, Indian Institute of Technology Bombay, Powai, Mumbai 400076, India

Supporting Information

ABSTRACT: Combretastatin A-4 (CA-4) in phosphate and serine pro-drug forms is under phase II clinical trials. With our interest of discovering CA-4 inspired new chemical entities, a novel series of 4,5-diaryl-2-aminoimidazole analogues of the compound was designed and synthesized by an efficient and diversity feasible route involving atom economical arene C−H bond arylation. Interestingly, four compounds showed potent cell-based antiproliferative activities in nanomolar concentrations. Among the compounds, compound **12** inhibited the proliferation of several types of cancer cells much more efficiently than CA-4. It depolymerized microtubules, induced spindle defects, and stalled mitosis in cells. Compound **12** bound to tubulin and inhibited the polymerization of tubulin in vitro. In addition, podophyllotoxin and CA-4 inhibited the binding of compound **12** to tubulin. The distinctive pharmacophoric features of the bridging motif as well as quinoline nucleus were explored. We noted also a valuable quality of compound **12** as a potential probe in characterizing new CA-4 analogues.

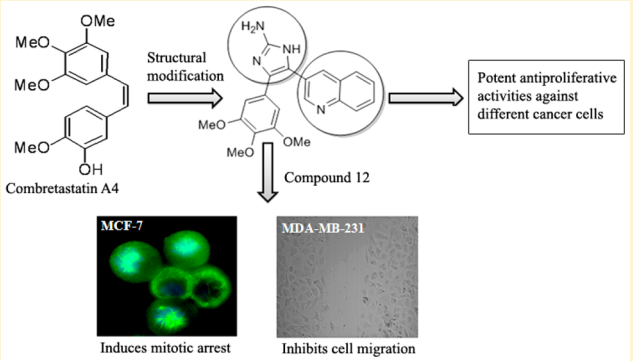

INTRODUCTION

Microtubules are critical elements in diverse cellular functions such as mitosis and cell motility. Some of the microtubule-targeting agents have been found to be clinically successful for the treatment of cancer, and therefore, microtubules are considered to be attractive anticancer drug targets.[1−3] Microtubule perturbing agents either enhance or inhibit the assembly of microtubules. For example, taxane ligands stimulate microtubule polymerization whereas vinca alkaloids and colchicine are known to induce depolymerization of microtubules.[4,5] Several natural ligands bind to the colchicine-binding site of tubulin and some of them are structurally similar; for example, combretastatin,[6] podophyllotoxin,[7] and steganacin[8] (Figure 1A). All these agents comprise common structural features, a 3,4,5-trimethoxyphenyl (TMP) moiety and the *cis*-locking of two aryl groups, which have been found to be crucial in inhibiting tubulin polymerization and antiproliferative activities.[9] These distinctive simple structural features have triggered many medicinal chemistry programs to focus on structural modulation of naturally potent ligands, especially combretastatin A-4 (CA-4), toward the discovery of potent antitubulin agents.

Combretastatins belong to the stilbenoid phenol class of compounds isolated from the bark of an African willow tree named *Combretum caffrum*.[10] In combretastatin family, combretastatin A-4 is the most active member, which strongly inhibits tubulin assembly by interacting at the colchicine-binding site.[11] CA-4 reversibly binds at the colchicine-binding site of tubulin, whereas the binding of colchicine to tubulin is a poorly reversible process.[12] Importantly, most of the tubulin inhibitors that target colchicine-binding site have been found to display vascular disruption and CA-4 was found to be a potent agent for rapid disruption of endothelial cell morphology in tumor capillaries responsible for limited blood flow and thus causing tumor cell death.[13,14] CA-4 is a poorly water-soluble compound. Its 3-*O*-phosphate prodrug form (CA-4-P, Zybrestat)[15] and serine amino acid analogue of CA-4 (AVE8062)[16] and combretastatin A-1 2,3-*O*-diphosphate (CA-1-P, OXi4503)[17] (Figure 1B), which are water-soluble, are currently under clinical trials both as a single drug and in combination for anticancer therapy. CA-4 possesses a short biological half-life[18]

Received: January 22, 2016

 © XXXX American Chemical Society

DOI: 10.1021/acs.jmedchem.6b00101
J. Med. Chem. XXXX, XXX, XXX−XXX

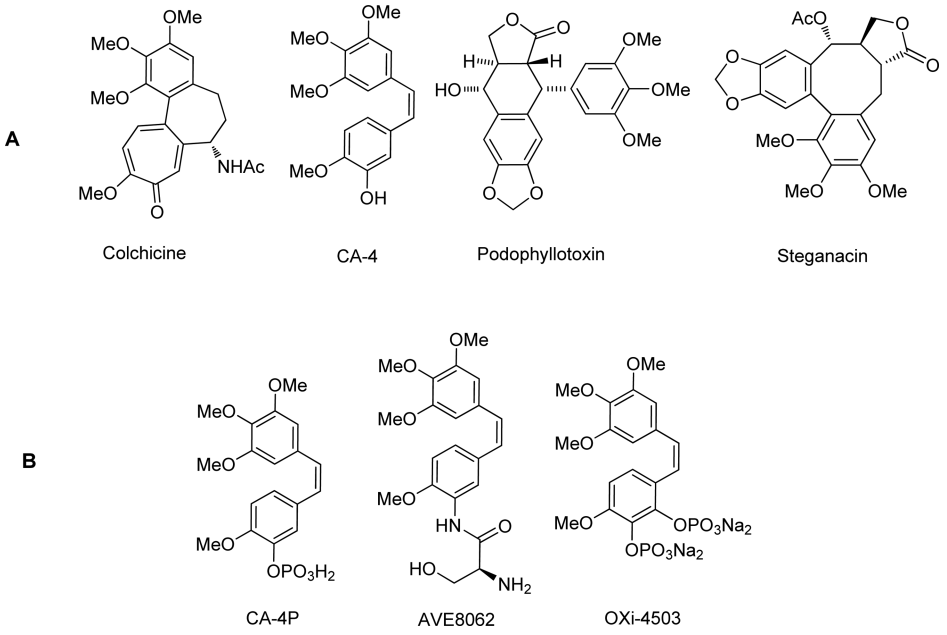

Figure 1. Structures of (A) natural products and (B) clinical trial agents which bind at the colchicine-binding site of tubulin.

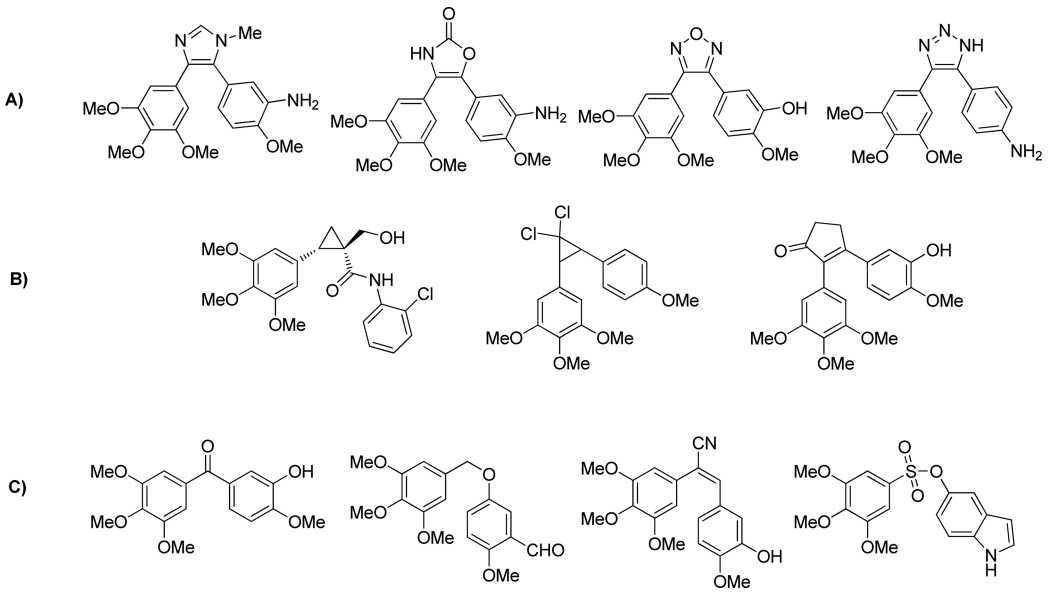

Figure 2. Some representative examples for replacement of double bond: (A) heterocyclic, (B) carbocyclic, and (C) functional bridging moieties.

and undergoes isomerization of a stilbenic olefin from an active *cis*-isomer to an inactive *trans*-isomer in the presence of light, heat, or protic media[19] and in physiological conditions.[20] In recent years, efforts have been made to overcome these limitations by derivatization of double bond and the hydroxyl substituent in ring B. To maintain the *Z*-geometry of two aryl rings, introduction of various linkers in place of double bond have been considered, for example, heterocyclic rings including imidazole,[16] 2(5*H*)-furanone,[21] oxazolone,[22] 4-arylcoumarin,[23] furazan,[24] triazole,[25] dihydroisoxazole,[26] 2-aminothiazole,[27] tetrazole,[28] and indole,[29] and carbocyclic rings including cyclopropane[30] and cyclopentenone[31] (Figure 2). The maintenance of (*Z*)-stilbene geometry is also known via introducing a variety of bridging functional groups, such as a ketone,[32] sulfide,[33] ether,[34] nitrile,[35] and sulfonate[36] (Figure 2). As a part of our research activities focused on the natural product based anticancer drug discovery,[37] we developed recently novel 2-aryl-3-arylamino-imidazo-pyridine/pyrazine antitubulin anticancer agents.[38]

In this direction, we envisaged that the replacement of the double bond in CA-4 with a 2-aminoimidazole skeleton that can provide additional features of multipoints hydrogen bond donors/acceptors by C2-amino and ring N/NH functionalities for interaction with tubulin (Figure 3). In addition, it may provide the drug-like physicochemical properties including aqueous solubility. Indeed, 2-aminoimidazole is a valuable molecular motif in medicinal chemistry, as proven by its presence in a wide range of bioactive marine natural products,[39] such as oroidin,[40] bromoageliferin,[41] sceptrin,[42] ageliferin,[43] CAGE,[44] and TAGE.

In the investigated 2-aminoimidazole series of compounds, 3,4,5-trimethoxyphenyl moiety as ring A (4-position) and

DOI: 10.1021/acs.jmedchem.6b00101
J. Med. Chem. XXXX, XXX, XXX−XXX

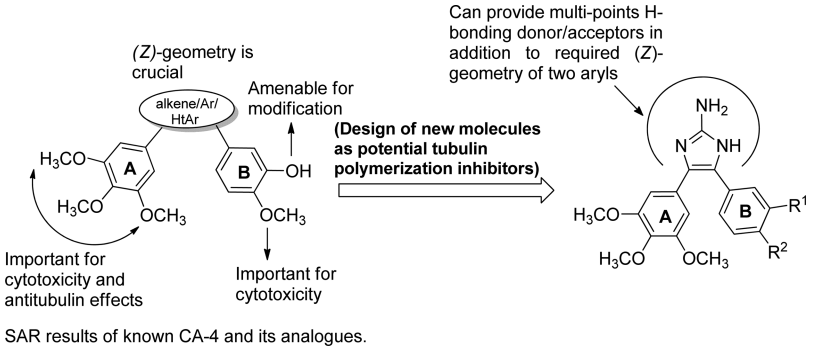

Figure 3. Design of novel 4,5-diaryl-2-aminoimidazoles as potential antitubulin and anticancer agents.

various relevant (hetero)aryls as ring B (5-position) were considered. Interestingly, four of the investigated 2-amino-imidazole analogues of CA-4 exhibited nanomolar antiproliferative activities. One compound (**12**) displayed significantly more potent antiproliferative activity against human breast adenocarcinoma (MCF-7), cervical cancer (HeLa), hepatocellular carcinoma (HuH-7), highly metastatic breast cancer (MDA-MB-231), and drug resistant mouse mammary tumor (EMT6/AR1) than CA-4. It strongly perturbed the organization of both interphase and mitotic microtubules and blocked the progression of the cells in mitosis. The compound inhibited tubulin assembly via binding at the colchicine site. Interestingly, compound **12** displayed strong fluorescence upon binding to tubulin. Furthermore, podophyllotoxin and CA-4 were able to displace compound **12** from the tubulin−compound **12** complex indicating that compound **12** binds to tubulin reversibly. This provides a unique opportunity to use it as a probe in characterizing new inhibitors of tubulin. The structure antitubulin/proliferative activity relationship and the important pharmacophoric features have been explored.

RESULTS AND DISCUSSION

Chemistry. Our designed 2-amino-imidazole class of compounds possess relevant functionalized/substituted two aryl moieties at 4 and 5 positions, and one of the aryls is 3,4,5-trimethoxyphenyl. A survey of the literature revealed that 4,5-disubstituted 2-amino-imidazoles were, in general, prepared by a classical reaction of benzil[45] or benzoin[46] with guanidine. The reaction[47] of α-haloketone with *N*-acetylguanidine followed by deacetylation, and the reaction of α-aminoketone with cyanamide leading to 2-amino-imidazoles are also known.[48] However, all these methods are limited to preparation of symmetrical 4,5-diaryl or 4,5-aryl/alkyl substituted 2-aminoimidazoles only. In addition, to prepare our designed compounds in these methods, the starting compounds would be benzil/benzoin, α-haloketone, or α-aminoketone and should possess 3,4,5-trimethoxyphenyl at one end and relevant substituted aryl group at other, which are difficult to access. These constraints impelled development of a convenient and diversely feasible method for preparation of our designed compounds. Recently, hydrazine-mediated cleavage of imidazo[1,2-*a*]pyrimidine scaffold leading to the formation of 2-aminoimidazole has been demonstrated.[49] This encouraged us to envisage a new route to access our desired set of unsymmetrical relevant 4,5-diaryl substituted 2-aminoimidazoles. The preparation of 2-aryl-imidazo[1,2-*a*]pyridine by cyclocondensation of 2-aminopyridine with versatile bis/monoelectrophilic reactants are widely known, but surprisingly, the methods were rarely investigated for the synthesis of 2-aryl-imidazo[1,2-*a*]pyrimidine. In our initial studies for synthesizing intermediate imidazo[1,2-*a*]pyrimidine, we investigated several methods known for preparation of imidazo[1,2-*a*]pyridines (Scheme 1).

In method 1, a $FeCl_3$-catalyzed reaction[50] of 2-amino-pyrimidine with nitrostyrene was performed. However, the formation of the desired product that required cascade transformations of Michael addition, intramolecular nucleophilic substitution, and dehydronitration were not observed. Increasing the catalyst quantity and variation in solvent did not promote the reaction, plausibly due to the poorly nucleophilic nature of 2-aminopyrimidine. In method 2, a reaction of 2-aminopyrimidine with 2-bromoacetophenone in the presence of sodium bicarbonate was done.[51] The desired product formed, but the conversion was found to be less and side products formed on prolonging the reaction. In method 3, the cyclo-condensation reaction of 2-aminopyrimidine with acetophenone via imine formation followed by tandem intramolecular C−H amination catalyzed by $Cu(OAc)_2$ and ZnI_2 was done following a method reported for 2-aminopyridine.[52] The desired product formed in moderate yield, although the reaction was incomplete. Variation in Cu catalyst, solvent, and temperature did not improve the yield considerably. In the next step, selective C-3 arylation of imidazo[1,2-*a*]pyrimidine was investigated with bromobenzene. The Pd-catalyzed selective direct C3−H arylation of 2-unsubstituted imidazo [1,2-*a*]pyridines with aryl halides is known.[53] We followed the method for the direct C3-arylation of C-2 substituted imidazo [1,2-*a*]pyrimidine (route 1). However, much less conversion was observed. With increased quantity of $Pd(OAc)_2$-precatalyst (5 mol %), the desired product was obtained in high yield. In the next step, 2,3-diaryl-imidazopyrimidine was subjected to cleavage of fused pyrimidine ring by using 20% ethanolic hydrazine under microwave-assisted dielectric heating. Following this protocol, final compounds **1**, **2**, **3**, **4**, **5**, **6**, **8**, **10**, **11**, **12**, and **13** with relevant (hetero) aryl substitutions were synthesized (Figure 4).

While this route was applied to the synthesis of compounds **7**, **9**, and **14**, corresponding arylation reactions were found to be low-yielding. Therefore, they were prepared by another method (route 2, Scheme 1). In this method (route 2, Scheme 1), C3 bromination of imidazo[1,2-*a*]pyrimidine by NBS followed by Suzuki coupling with arylboronic acids were done, which provided the desired products 2,3-diarylimidazo-pyrimidine in comparative yield. For the synthesis of compound **15**, a direct C3 arylation of 2-(3,4,5-trimethoxyphenyl)-imidazopyrimidine with 5-bromo-2-methoxyphenol using

DOI: 10.1021/acs.jmedchem.6b00101
J. Med. Chem. XXXX, XXX, XXX−XXX

Scheme 1. Synthesis of Investigated Compounds (1−15)

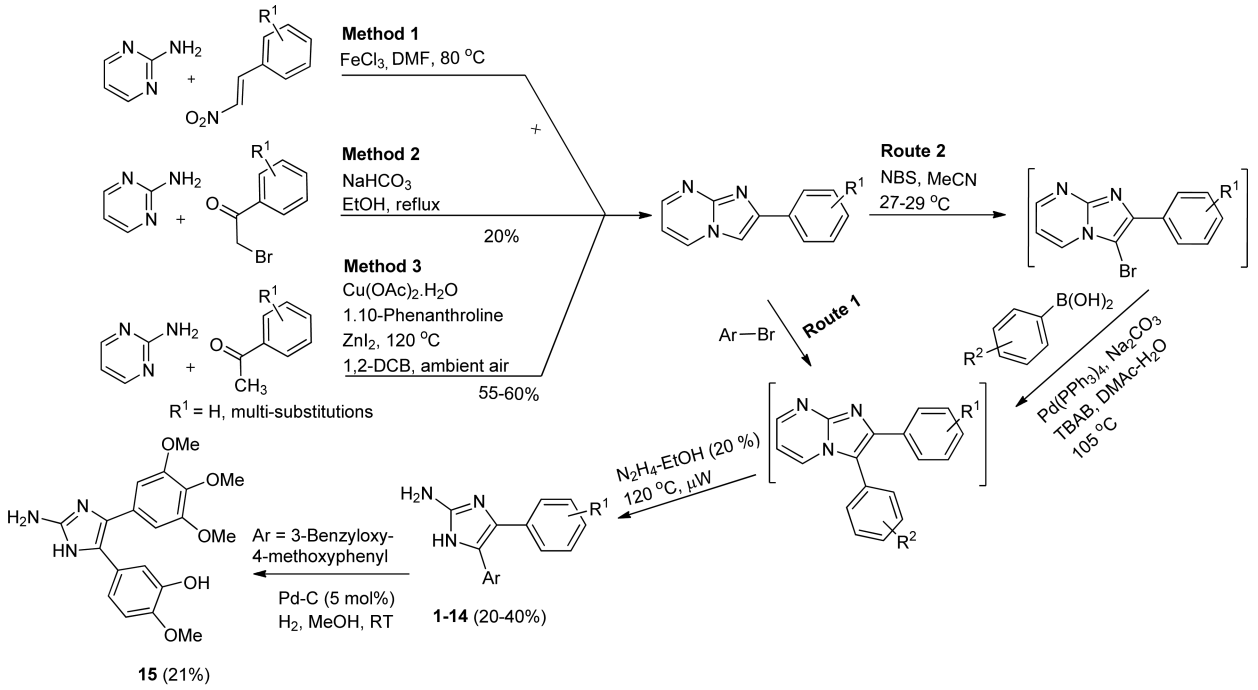

Route 1; $Pd(OAc)_2$, KOAc, DMAc, 150 °C: For Ar-Br = 2-(benzyloxy)-4-bromo-1-methoxybenzene; $Pd(OAc)_2$, Cs_2CO_3, Ph_3P, 1,4-dioxane, 160 °C, μW, Ar

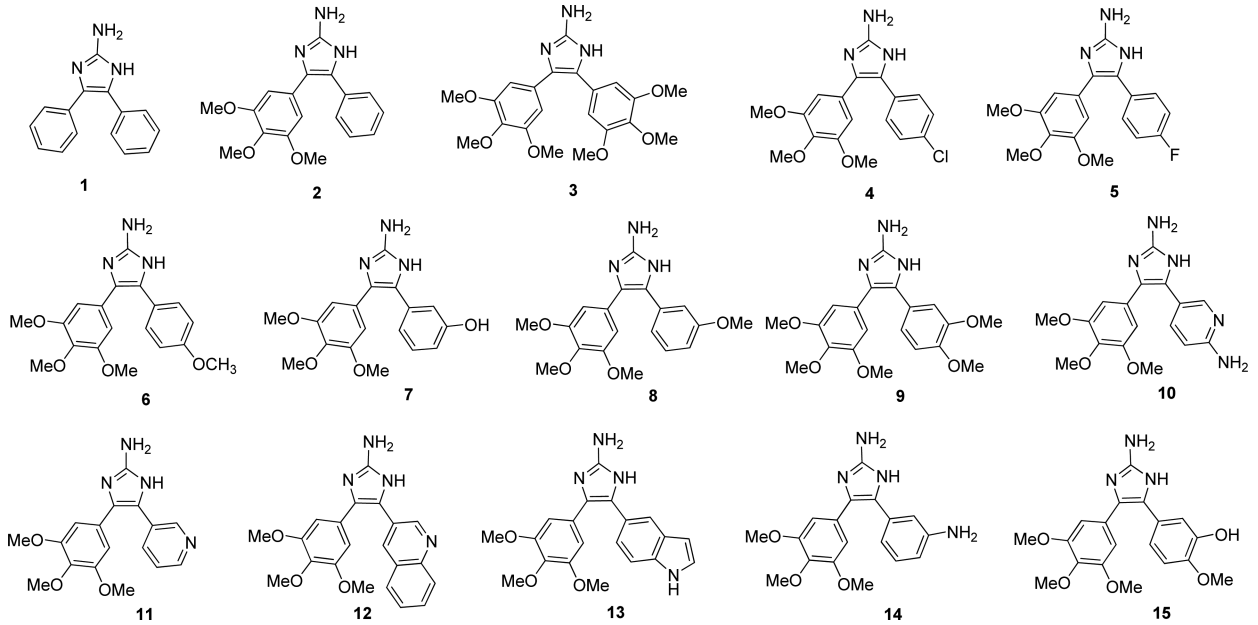

Figure 4. Synthesized 4,5-biarylated-2-aminoimidazoles (**1−15**).

optimized reaction conditions did not occur. The protection−deprotection chemistry was then applied. The hydroxyl group of 5-bromo-2-methoxyphenol was protected as a benzyloxy moiety by reaction with benzyl bromide.[54] After several experiments, the arylation with 2-(benzyloxy)-4-bromo-1-methoxybenzene was found to be successful with a reported method[55] with some modifications such as an increase in the catalyst, base, and ligand. After C3-arylation, the hydrazine mediated ring cleavage and subsequent debenzylation by classical Pd−C catalyzed hydrogenation provided desired compound (**15**) (Scheme 1). The structures of the compounds (**1−15**) were characterized by ^{1}H and ^{13}C NMR (Supporting Information).

Biological Studies. *Cell-Based Screening of Combretastatin Analogues for Their Antiproliferative Activity.* Combretastatin analogues (**1−15**) were screened in HeLa and MCF-7 cell lines using sulforhodamine assay (Table 1). CA-4 was used as a control to make a comparison of the potency of the synthesized combretastatin analogues. The half-maximal inhibitory concentration (IC_{50}) for all the compounds (**1−15**) tested against MCF-7 and HeLa cells is shown in Table 1. Of the enlisted compounds, four compounds, namely compound

DOI: 10.1021/acs.jmedchem.6b00101
J. Med. Chem. XXXX, XXX, XXX−XXX

Table 1. Half-Maximal Inhibitory Concentration of Synthesized Combretastatin Analogues in MCF-7 and HeLa Cell Line

combretastatin analogues	IC_{50} in MCF-7 (nM)	IC_{50} in HeLa (nM)
1	187 ± 5	197 ± 3
2	(27 ± 12) × 10^3	(34 ± 14) × 10^3
3	(12 ± 4) × 10^3	(8 ± 7.7) × 10^3
4	(8 ± 2) × 10^3	(3 ± 2) × 10^3
5	(3 ± 1) × 10^3	(3.4 ± 3) × 10^3
6	174 ± 7	166 ± 9
7	(53 ± 24) × 10^3	(18 ± 12) × 10^3
8	(18 ± 7) × 10^3	(14 ± 7) × 10^3
9	71 ± 6	68 ± 2
10	(21 ± 3) × 10^3	(18 ± 2) × 10^3
11	(13 ± 6) × 10^3	(4 ± 1) × 10^3
12	3 ± 2	10 ± 1
13	(8 ± 6) × 10^3	(3 ± 2) × 10^3
14	(6 ± 4) × 10^3	(8 ± 3) × 10^3
15	220 ± 12	390 ± 21
CA-4	18 ± 2	25 ± 2

12, **9**, **6**, and **1**, were found to potently inhibit the proliferation of MCF-7 and HeLa cells. Because compound **12** was found to be the most potent among the tested combretastatin analogues, and therefore the antiproliferative activity of compound **12** was further characterized.

A structure−activity relationship was established based on the variation of the ring B in compounds (**1**−**15**) tested for antiproliferative activities in MCF-7 and HeLa cell line. The presence of 4-methoxy- or 3,4-dimethoxy-phenyl as ring B provided very good antiproliferative activities. On the other hand, 2-aminopyridine or pyridine as ring B showed poor activities. Moderate activities were shown by compounds that contain ring B moieties, 3,4,5-trimethoxyphenyl, 4-chloro/fluoro-phenyl, 3-methoxyphenyl, aniline, or indole. The compound containing quinoline as ring B was found to be most potent antiproliferative and superior effective than CA-4.

*Effect of Compound **12** on the Cell Proliferation in Cancer Cell Lines.* Compound **12** inhibited the proliferation of MCF-7 and HeLa cells with a half-maximal inhibitory concentration (IC_{50}) at 3 ± 2 and 10 ± 1 nM, respectively (Figure 5A,B). CA-4 inhibited the proliferation of MCF-7 and HeLa cells with an IC_{50} value of 18 ± 2 and 25 ± 2 nM, respectively (Figure 5C and 5D). The results indicated that compound **12** displayed more potent antiproliferative effects against MCF-7 and HeLa cells than CA-4. Compound **12** also inhibited the proliferation of highly metastatic breast cancer cells (MDA-MB-231), drug resistant mouse mammary cancer cells (EMT6/AR1), and hepatocarcinoma cells (HuH-7) more potently than CA-4 (Table 2). On the basis of structure−activity relationships and the superior antiproliferative activities (Tables 1 and 2) of most of the investigated class of compounds compared to CA-4 in multiple cancer cell lines (MCF-7, HeLa, MDA-MB-231, EMT6/AR1, and HuH-7), it is evident that the 2-amino-imidazole skeleton bridging two aryls (A and B), as replacement of double bond in the CA-4, and the quinoline as ring B are important pharmacophoric features in addition to trimethoxyphenyl as ring A. This may be plausibly due to the biological target−ligand interaction stabilized by hydrogen bonding with ring N/NH and C2-amine functionalities of 2-aminoimidazole and quinoline N in the ligand.

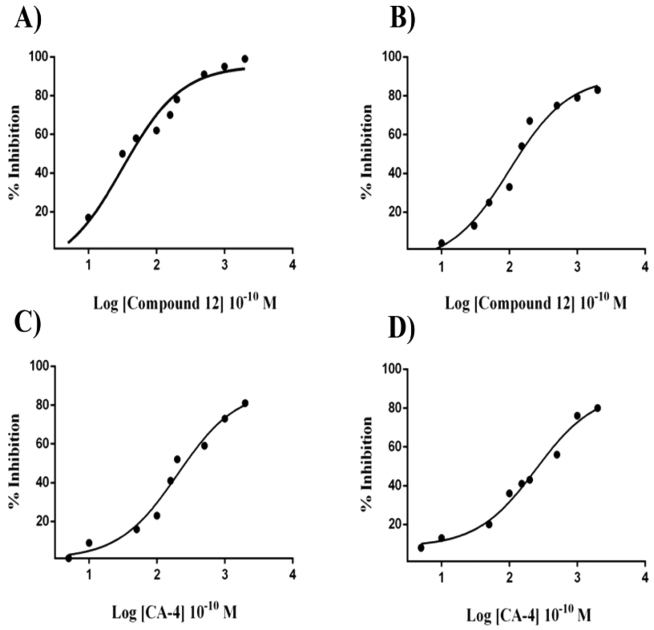

Figure 5. Compound **12** and CA-4 inhibited the proliferation of MCF-7 and HeLa cells. Effects of compound **12** in MCF-7 (A) and HeLa (B) and the effects of CA-4 in MCF-7 (C) and HeLa (D) are shown.

Table 2. Half-Maximal Inhibitory Concentration of Compound 12 and CA-4 in Different Tumor Cell Lines

cell lines	**12** (nM)	CA-4 (nM)
MDA-MB-231	96 ± 13	331 ± 32
EMT6/AR1	350 ± 7	495 ± 11
HuH-7	335 ± 10	430 ± 9

*Compound **12** Depolymerized Microtubules and Caused Mitotic Block in MCF-7 Cells.* Combretastatins are known to depolymerize cellular microtubules. Compound **12** also found to depolymerize microtubules in a concentration-dependent manner. For example, 5 nM compound **12** depolymerized interphase microtubules moderately whereas 10 nM compound **12** induced strong depolymerization of interphase microtubules in MCF-7 cells (Figure 6).

Further, compound **12** also perturbed the mitotic spindles. At concentrations above 5 nM of compound **12**, monopolar spindles were observed and the cells were found to be blocked in mitosis (Figure 7). A flow cytometry analysis of MCF-7 cells treated with 5 and 10 nM compound **12** indicated that 40 and 74% of the cells were in the G2/M phase, respectively (Table 3). Whereas in comparison, 20 and 46% of the cells were in the G2/M phase in the presence of 5 and 10 nM CA-4, respectively (Figure 8). To further corroborate the results, phosphohistone H3 (Ser-10) staining of the cells was performed. Phosphohistone H3 (Ser-10) is a mitotic marker of cells. The number of phosphohistone-stained cells increased in a concentration-dependent manner as compared to the vehicle-treated cells (Figure 9). The percentage of the mitotic cells was determined to be 8 ± 1, 15 ± 2, and 26 ± 1% in the absence and presence of 5 and 10 nM compound **12**, respectively.

*Compound **12** Inhibited the Migration of MDA-MB-231 Cells.* Combretastatins are well-known antivascular agents. Therefore, the effect of compound **12** on the wound closure of migratory tumor cells, MDA-MB-231 was evaluated.

DOI: 10.1021/acs.jmedchem.6b00101
J. Med. Chem. XXXX, XXX, XXX−XXX

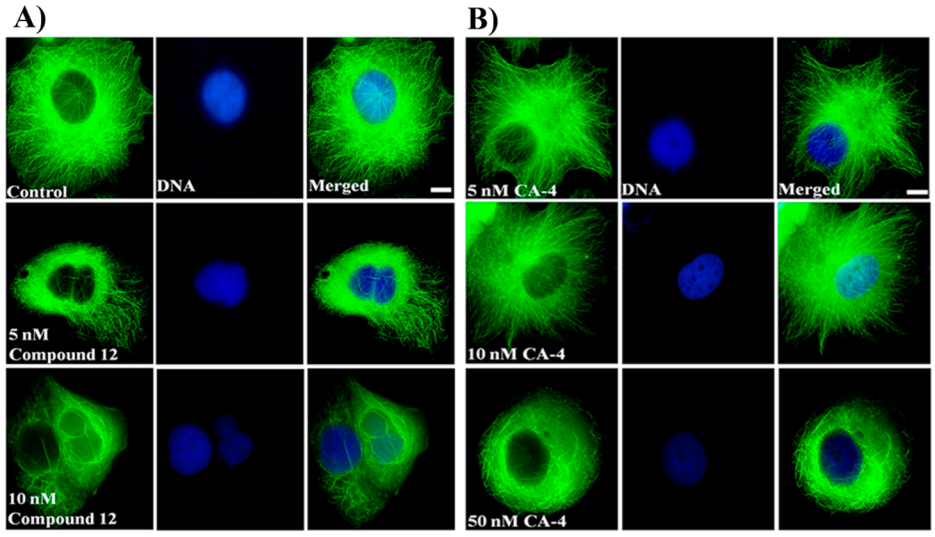

Figure 6. Compound **12** showed stronger depolymerizing effects on the interphase microtubule network than CA-4. MCF- 7 cells were incubated in the absence and presence of 5 and 10 nM of compound **12** (A) and 5, 10, and 50 nM of CA-4 (B) for 24 h. Cells were fixed and stained for α-tubulin (green) and nuclear stain, Hoechst (blue). Scale bar is 1 μm.

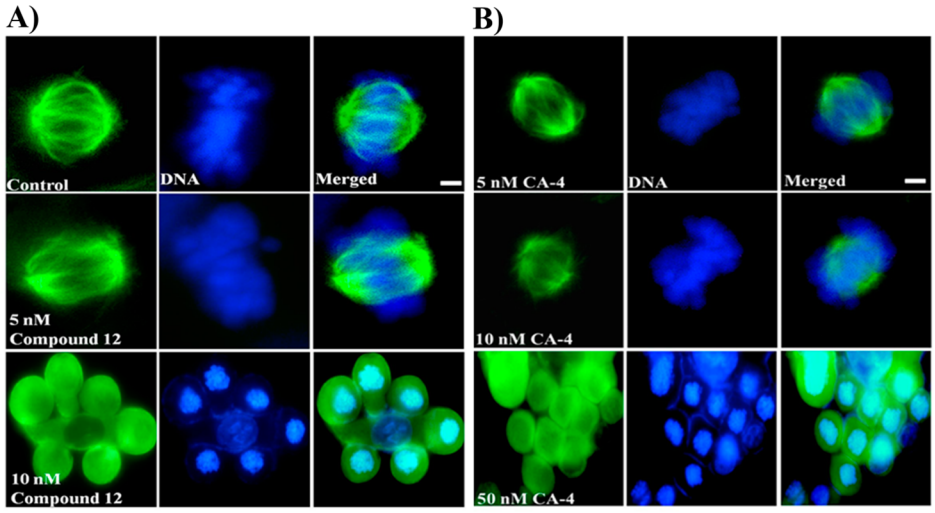

Figure 7. Effects of compound **12** and CA-4 on the mitotic spindles in MCF-7 cells. (A) MCF-7 cells were incubated either with the vehicle or with 5 and 10 nM compound **12** (A) and 5, 10, and 50 nM CA-4 (B) for 24 h and stained for α-tubulin (green) and nuclear stain, Hoechst (blue). Scale bar is 1 μm.

Table 3. Percentage of MCF-7 Cells after Treatment with Compound 12 and CA-4 and Analyzed by Flow Cytometry

compd	G1	S	G2/M
control	49	35	16
12 (5 nM)	34	25	40
12 (10 nM)	16	10	74
CA-4 (5 nM)	51	23	26
CA-4 (10 nM)	41	16	43
CA-4 (50 nM)	14	23	63

The wound was completely closed after 18 h in control cells (Figure 10). CA-4 (50 nM) showed a minimal (8 ± 1%) inhibitory effect on cell migration, while 50 nM compound **12** inhibited the wound healing by 56 ± 3% and 150 nM of CA-4 inhibited the wound healing by 52 ± 4%. The finding indicated that compound **12** strongly inhibits the migration of MDA-MB-231cells than CA-4.

*Compound **12** Inhibited the Polymerization of Tubulin in Vitro.* Because compound **12** depolymerized microtubules in cells, the effect of compound **12** on the assembly kinetics of tubulin was analyzed in vitro. Compound **12** inhibited the rate and extent of the assembly of tubulin in a concentration-dependent manner (Figure 11A) and the half-maximal inhibition (IC_{50}) of tubulin assembly occurred in the presence of 1.6 ± 0.7 μM of the compound. The results indicated that compound **12** is a potent inhibitor of tubulin assembly. Compounds **9** and **6** were found to inhibit the tubulin assembly with an IC_{50} of 11 ± 1 and 13 ± 2 μM, respectively (Figure 11B,C). Under similar conditions, CA-4 inhibited the assembly of tubulin with an IC_{50} of at 1.7 ± 0.1 μM (Figure 11D). Compound **1** (20 μM) did not have a significant inhibitory effect on the assembly of tubulin.

*Determination of the Dissociation Constant of Compound **12** to Tubulin in Vitro.* Compound **12** inhibited the assembly of tubulin. Therefore, we analyzed its binding with

DOI: 10.1021/acs.jmedchem.6b00101
J. Med. Chem. XXXX, XXX, XXX−XXX

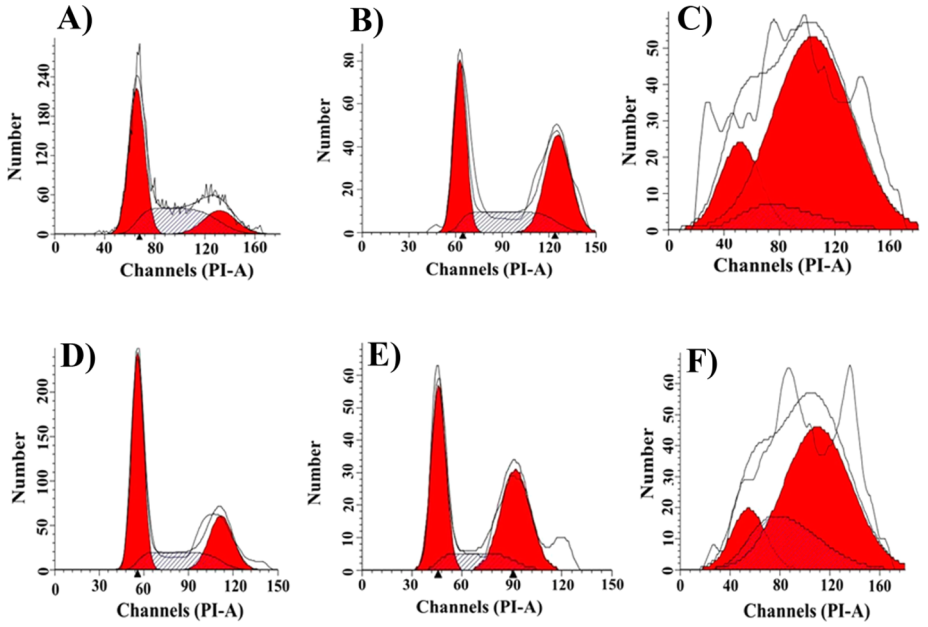

Figure 8. Compound **12** increased the percentage of cells in the G2/M phase. MCF-7 cells were incubated with either in the absence (A) or in the presence of 5 (B) and 10 (C) nM compound **12** and 5 (D), 10 (E), and 50 (F) nM CA-4 for 24 h. The flow cytometry analysis was performed by staining the DNA with propidium iodide.

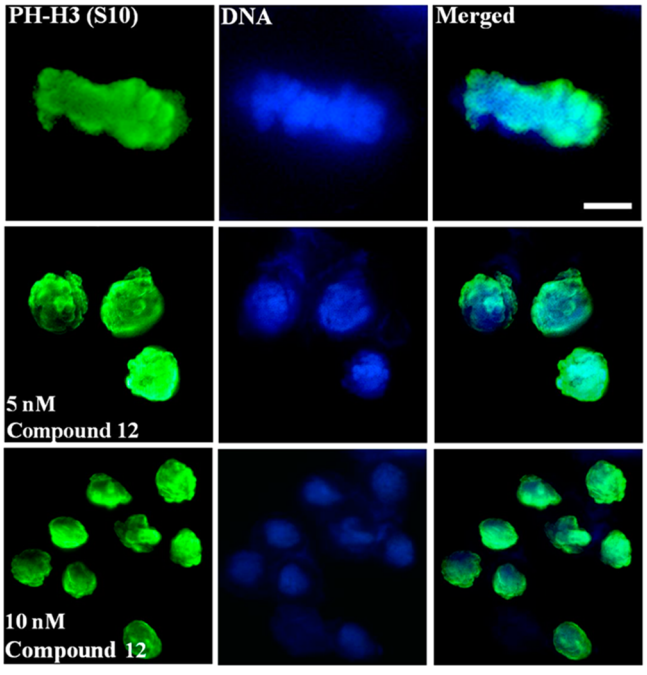

Figure 9. Compound **12** increased the number of phosphohistone stained cells. MCF-7 cells were incubated in the absence and presence of 5 and 10 nM compound **12** for 24 h and stained for phosphohistone (green) and nuclear stain Hoechst (blue). Scale bar is 10 μm.

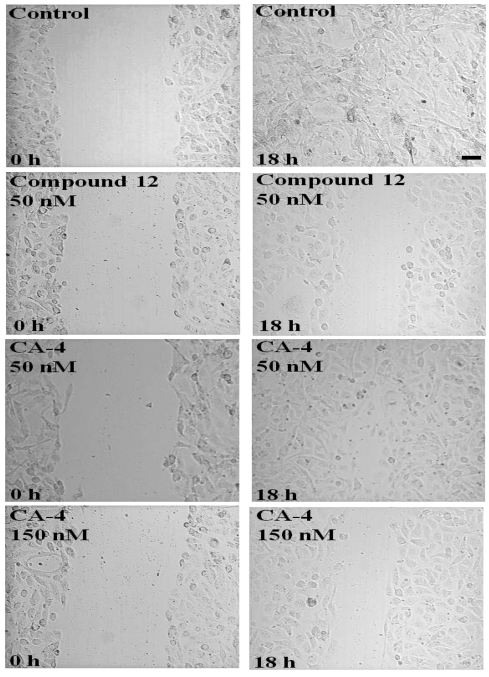

Figure 10. Compound **12** inhibited MDA-MB-231 cell migration. Effects of compound **12** and CA-4 on the wound closure are shown. Scale bar is 1 μm.

tubulin. Compound **12** quenched the fluorescence intensity of tubulin in a concentration-dependent fashion, indicating that it interacts with tubulin (Figure 12A). The fluorescence intensity changes were fitted in a binding isotherm to obtain a dissociation constant (K_d) for the binding of compound **12** to tubulin (Figure 12 B). The K_d was calculated to be 1.9 ± 0.3 μM.

*Determination of the Binding Site of Compound **12** on Tubulin.* Compound **12** displayed very low fluorescence intensity in aqueous solution (Figure 13). Interestingly, the fluorescence intensity of compound **12** increased several fold in the presence of tubulin, indicating that it formed a complex with tubulin (Figure 13).

Podophyllotoxin and CA-4 are known to bind to the colchicine site on tubulin.[56,57] Therefore, the binding site of compound **12** on tubulin was monitored by performing a competition experiment using podophyllotoxin as well as CA-4. The preincubation of podophyllotoxin with tubulin reduced the development of compound **12** fluorescence intensity in a

DOI: 10.1021/acs.jmedchem.6b00101
J. Med. Chem. XXXX, XXX, XXX−XXX

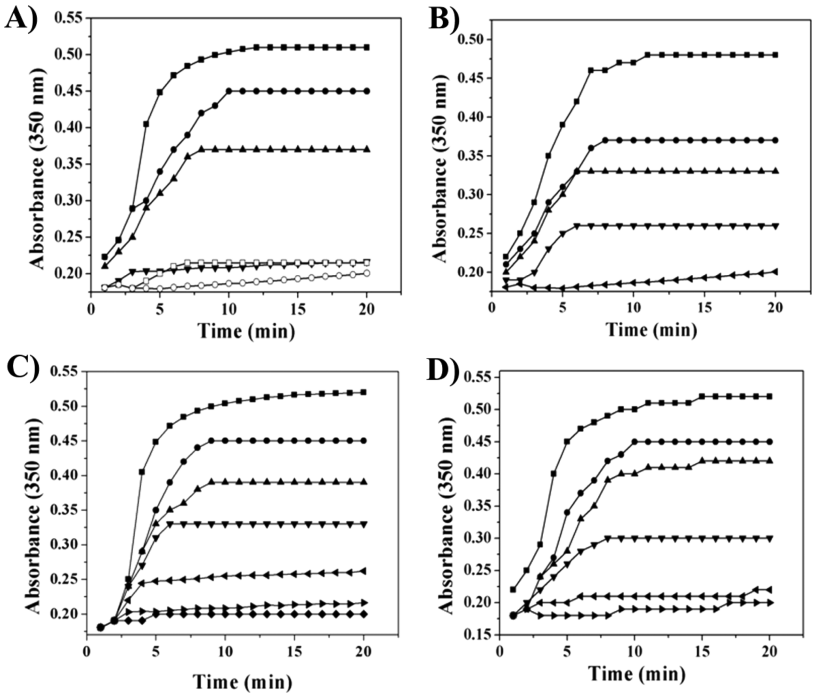

Figure 11. Compounds **12**, **9**, **6**, and CA-4 inhibited the assembly of tubulin in vitro. Tubulin (12 μM) was polymerized in the presence of 1 mM GTP and 1 M glutamate without (■) or with different concentrations 0.5 (●), 1 (▲), 2 (▼), 3 (□), and 5 (○) μM of compound **12** (A), different concentrations 5 (●), 10 (▲), 15 (▼), and 20 (◀) μM of compound **9** (B), different concentrations 5(●), 10(▲), 15(▼), 20 (◀) and 30 (▶) and 40 μM (◆) of compound **6** (C), and different concentrations 0.5(●), 1(▲), 2(▼), 3 (◀), and 5 (▶) μM of CA-4 (D). Three independent sets of experiments were performed for each compound. One of the sets is shown of all the experiments.

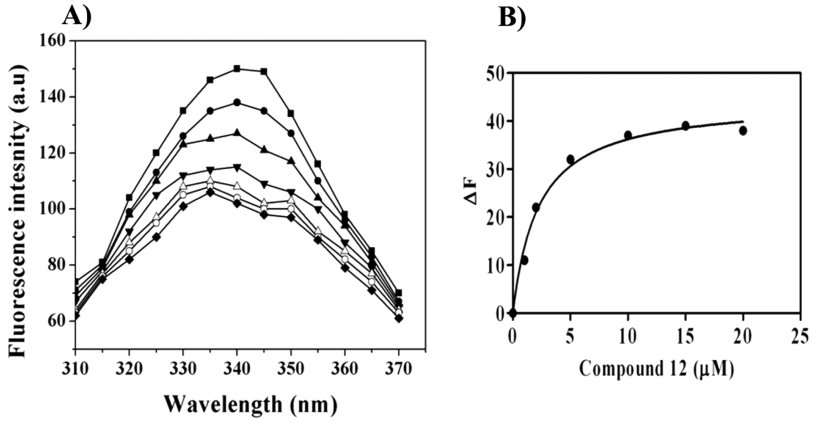

Figure 12. Compound **12** reduced the intrinsic tryptophan fluorescence of tubulin. (A) Tubulin (2 μM) was incubated without (■) and with different concentrations of 1 (●), 2 (▲), 5 (▼), 10 (Δ), 15 (○) and 20 (◆) μM of compound **12** in 25 mM PIPES buffer, pH 6.8, for 10 min at 25 °C. (B) The change in fluorescence intensity of tubulin upon binding with compound **12** was plotted. The experiment was conducted four times. One of the four sets is shown.

concentration-dependent manner (Figure 14A). A K_i value was determined to be 0.3 ± 0.14 μM (Figure 14B). Similarly, CA-4 reduced the binding of compound **12** to tubulin in a concentration dependent fashion (Figure 14C), and the K_i value was found to be 0.68 ± 0.7 μM (Figure 14D).

In addition, we checked whether CA-4 and podophyllotoxin could displace tubulin bound compound **12**. Tubulin was first incubated with compound **12** for 30 min and then either CA-4 or podophyllotoxin was added to the reaction milieu for further 30 min. The addition of CA-4 and podophyllotoxin reduced the fluorescence of tubulin−compound **12** complex, indicating that the binding of compound **12** to tubulin is reversible (Supporting Information, Figure S1). Because the fluorescence of compound **12** strongly increases upon binding to tubulin and compound **12** reversibly binds to tubulin, compound **12** can be used as a probe to evaluate tubulin inhibitors that bind to the CA-4 site in tubulin. Then we checked whether vinblastine and paclitaxel could inhibit the binding of compound **12** with tubulin. Tubulin was incubated with either vinblastine or paclitaxel for 10 min. Then compound **12** was added to the reaction mixtures. Vinblastine and paclitaxel could not reduce the development of the fluorescence intensity of compound **12**, indicating that these agents did not inhibit the binding of compound **12** to tubulin (Supporting Information, Figure S2). The results together indicated that compound **12** binds at the colchicine-binding site of tubulin. Further, the findings

DOI: 10.1021/acs.jmedchem.6b00101
J. Med. Chem. XXXX, XXX, XXX−XXX

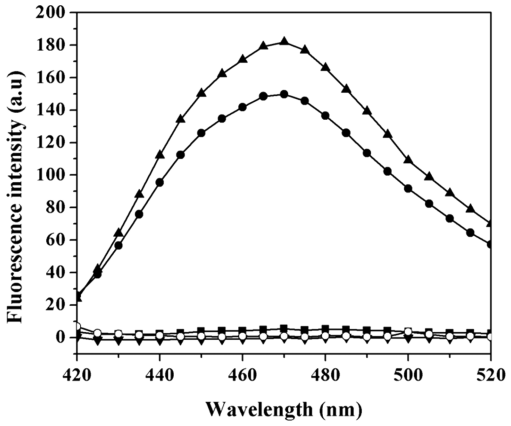

Figure 13. The fluorescence intensity of compound **12** increased in the presence of tubulin. Tubulin (2 μM) was incubated without (■) and with 5 (●) and 10 μM (▲) of compound **12** in 25 mM PIPES buffer for 10 min at 25 °C. The spectra of 5 (▼) and 10 (○) μM compound **12** were also monitored using 350 nm as the excitation wavelength.

indicated that compound **12** may be used to screen agents that bind to the colchicine site on tubulin in general and particularly for CA-4 analogues.

CONCLUSION

In conclusion, we designed a new series of analogues of combretastatin A-4, comprising 2-aminoimidazole as a bridging skeleton replacing a double bond in CA-4, 3,4,5-trimethoxyphenyl in ring A and various relevant (hetero) arenes in ring B. Fifteen compounds were synthesized by a diversity feasible and atom-economical route involving arene C−H bond arylation. Four compounds exhibited antiproliferative activities in nanomolar concentrations. 5-Quinolin-3-yl and 4-(3,4,5-trimethoxyphenyl) substituted imidazol-2-amine (compound **12**) was most potent. Compound **12** showed higher antiproliferative activity than CA-4 against five different cancer cell lines including a drug resistant cell line. In addition, compound **12** exerted stronger inhibitory effect on the migration of highly metastatic MDA-MB-231 than CA-4, indicating its strong antimetastatic potential. Compound **12** was found to cause a significant depolymerization and perturbation of the interphase and mitotic microtubule network and induced mitotic arrest in MCF-7 cells. Like CA-4, compound **12** inhibited the rate and extent of an in vitro assembly of purified tubulin with an IC_{50} of 1.6 μM. A dissociation constant of 1.9 μM is indicative of a strong binding affinity of compound **12** to tubulin. Importantly, compound **12** when bound to tubulin showed an increase in the fluorescence intensity, indicating its potential use as a probe

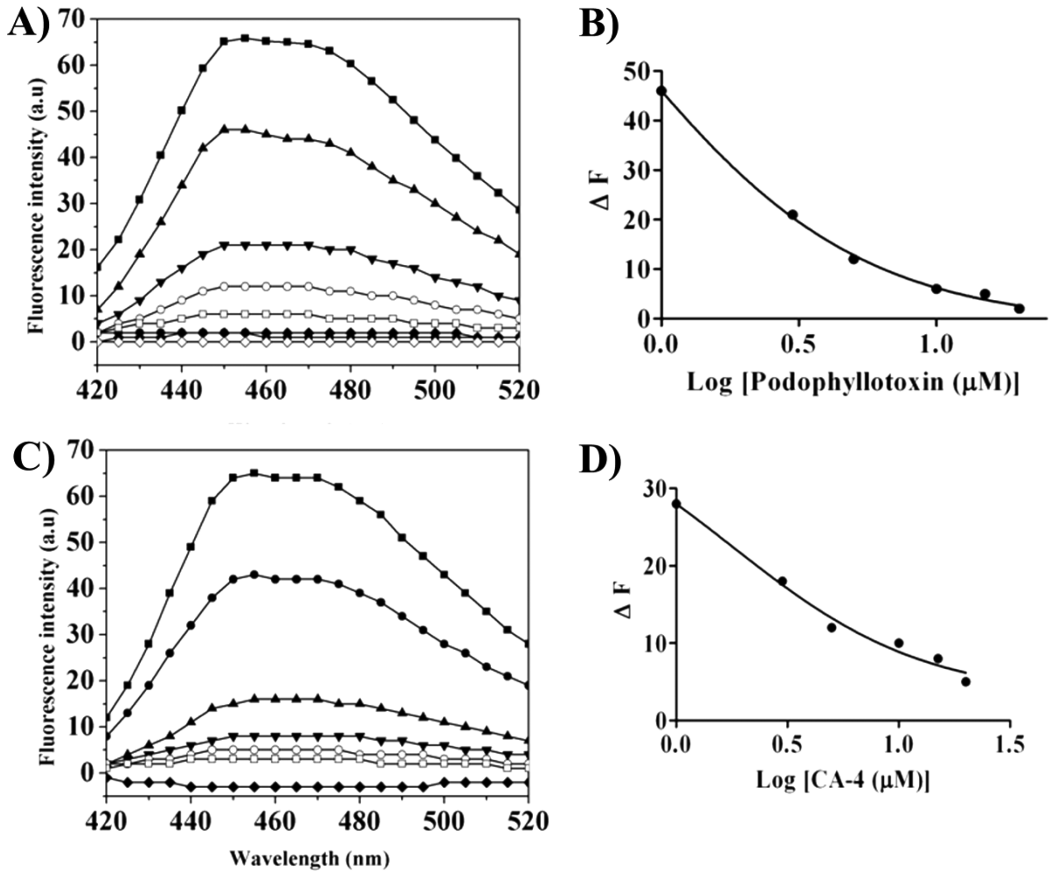

Figure 14. Compound **12** bound at the colchicine site on tubulin. (A) Tubulin (3 μM) was incubated without (■) or with different concentrations 1 (▲), 3 (▼), 5 (○), 10 (□), 15 (◆), and 20 μM (●) of podophyllotoxin in 25 mM PIPES for 15 min at 25 °C. Then, the reaction mixtures were incubated with 6 μM compound **12** for an additional 15 min at 25 °C. The spectrum of 6 μM (◇) compound **12** in the absence of tubulin is also shown. The experiment was performed three times. (B) The changes in the fluorescence intensities were plotted against different concentrations of podophyllotoxin. (C) Tubulin (3 μM) was incubated without (■) or with different concentrations of 1 (●), 3 (▲), 5 (▼), 10 (○), 15 (□), and 20 (◆) μM of CA-4 in 25 mM PIPES for 15 min at 25 °C. Subsequently, the reaction mixtures were incubated with 6 μM compound **12** for another 15 min at 25 °C. Three sets of experiments were performed. One of the sets is shown. (D) The change in fluorescence intensity was plotted against CA-4 concentrations.

DOI: 10.1021/acs.jmedchem.6b00101
J. Med. Chem. XXXX, XXX, XXX−XXX

in the characterization of new antitubulin agents. Competition studies with CA-4 and podophyllotoxin for tubulin-binding signified that compound **12** binds at the colchicine site on tubulin. The results indicated the importance of 2-amino-imidazole as bridging skeleton and quinoline motif in ring B in the structural modulation of CA-4 for generating a new class of antitubulin agents.

EXPERIMENTAL SECTION

Chemistry. *General Considerations.* All reactants and reagents were obtained from the commercial source and used without further purification. The NMR spectra were recorded on a Bruker Avance DPX 400 MHz spectrometer in $CDCl_3$/DMSO-d_6/CD_3OD solvents using TMS as an internal standard. *J* values are given in Hz. HRMS (ESI) were recorded with Bruker−Maxis mass spectrometers. IR spectra were recorded on a Nicolet FT−IR Impact 410 instrument as a thin film (neat). The reactions were monitored by TLC (Merck, Silica gel 60 F_{254}). The purity of synthesized compounds was analyzed by HPLC (Shimadzu LC-6AD system), Phenomenex RP-C18 column (250 mm × 4.60 mm), particle size 5 μm, flow rate 1 mL/min, using water−acetonitrile. 2-(Benzyloxy)-4-bromo-1-methoxybenzene was prepared following a known method.[54]

Synthesis of Compounds (1−15). *Representative Experimental Procedure for the Synthesis of Compound 2.* A mixture of 2-aminopyrimidine (114 mg, 1.2 mmol), 3,4,5-trimethoxyacetophenone (210 mg, 1.0 mmol), $Cu(OAc)_2{\cdot}H_2O$ (20 mg, 0.1 mmol), 1,10-phenanthroline (18 mg, 0.1 mmol), and zinc iodide (32 mg, 0.1 mmol) in 1,2-dichlorobenzene (2 mL) was stirred at 120 °C. After maximal conversion (24 h, monitored by TLC), the resultant mixture was washed by hexane to remove the solvent. The column chromatographic purification of crude mass on neutral alumina provided the intermediate 2-(3,4,5-trimethoxyphenyl)imidazo[1,2-*a*]-pyrimidine (157 mg, 55%). For C-3 direct arylation (route 1), intermediate 2-(3,4,5-trimethoxyphenyl)imidazo[1,2-*a*]pyrimidine (342 mg, 1.2 mmol) was stirred with bromobenzene (157 mg, 1 mmol), KOAc (196 mg, 2 mmol), and $Pd(OAc)_2$ (11.2 mg, 5 mol %) at 150 °C in DMAc (4 mL). After maximal conversion (24 h, monitored by TLC), solvent was evaporated under vacuum. The crude reaction mixture was extracted with EtOAc (2 × 40 mL) and washed with water (2 × 20 mL). The organic layer was dried with anhyd Na_2SO_4 and concentrated under vacuum, which provided intermediate 2,3-diarylated imidazopyrimidine. Then the resultant crude mixture without further purification was subjected to ring cleavage by heating with hydrazine hydrate (20% in methanol, 3 mL) under microwave irradiation at 120 °C. After completion of the reaction (15 min, monitored by TLC), the solvent was evaporated under vacuum. The column chromatographic purification of crude mass on silica gel provided compound **2** in 36% isolated yield (starting from intermediate 2-(3,4,5-trimethoxyphenyl)imidazo[1,2-*a*]pyrimidine). Compounds **1**, **2**, **3**, **4**, **5**, **6**, **8**, **10**, **11**, **12**, and **13** were prepared by following this procedure. For the synthesis of compounds **7**, **9**, and **14**, an alternative process (route 2) was followed. For bromination at C-3 position, 2-(3,4,5-trimethoxyphenyl)imidazo[1,2-*a*]pyrimidine (285 mg, 1 mmol) in methanol (2 mL) was stirred at 27−29 °C with small quantitywise addition of NBS (178 mg, 1 mmol). After complete conversion (1 h, monitored by TLC), the solvent was evaporated under vacuum. To this crude mixture were added DMAc−H_2O (1:1, 4 mL), arylboronic acid (1.3 equiv), Na_2CO_3 (530 mg, 5 equiv), TBAB (322 mg, 1 equiv), and $Pd(PPh_3)_4$ (115 mg, 0.1 mmol). The mixture was then refluxed with stirring at 105 °C. After completion of the reaction (monitored by TLC), a solvent mixture was evaporated under vacuum. The resultant mixture was extracted with EtOAc (2 × 40 mL) and washed with water (2 × 20 mL). The organic layer was dried with anhyd Na_2SO_4, and concentrated under vacuum. Then the resultant crude mixture of intermediate 2,3-diarylated imidazopyrimidine without further purification was subjected to ring cleavage following the process mentioned above. For the synthesis of compound **15**, arylation of 2-(3,4,5-trimethoxyphenyl)imidazo[1,2-*a*]pyrimidine (0.50 mmol, 145 mg) with 2-(benzyloxy)-4-bromo-1-methoxybenzene (198 mg, 1.35 equiv) was done following a reported method[55] with use of increased quantities of cesium carbonate (360 mg, 2.2 equiv), palladium acetate (33 mg, 15 mol %), and triphenylphosphine (40 mg, 30 mol %). Subsequently, the ring cleavage reaction was performed as described above. Finally, the benzyl deprotection was done in the presence of Pd−C in MeOH under H_2 gas. The crude reaction mixture was subjected to column chromatography on silica gel (60−120 mess size). Compound **15** was obtained in 21% overall yield starting from intermediate 2-(3,4,5-trimethoxyphenyl)imidazo[1,2-*a*]pyrimidine. The structures of investigated compounds (**1**−**15**) were characterized by ^1H and ^{13}C NMR, IR, and confirmed by HRMS (ESI). Their purity tested by HPLC were found to be >95%.

Materials and Methods. *Reagents.* Sulforhodamine B (SRB), mouse monoclonal, anti-α tubulin IgG as primary antibody, DABCO (1,4-diazabicyclo[2.2.2]octane), FITC conjugated antimouse IgG secondary antibody, and CA-4, Ethylene glycol-bis(2aminoethyl ether)-*N*,*N*,*N*′,*N*′-tetraacetic acid (EGTA) was purchased from Sigma (St Louis, MO, USA). Podophyllotoxin was procured from MP Biomedicals, India. Dulbecco's phosphate buffered saline (DPBS), Hoechst 33258, bovine serum albumin (BSA), piperazine-1,4-bis-2-ethanesulfonic acid (PIPES), magnesium chloride ($MgCl_2$), trichloroacetic acid (TCA), dimethyl sulfoxide, sodium bicarbonate, an antibiotic−antimycotic solution comprising of streptomycin, amphotericin B, and penicillin, and minimal essential media were purchased from HiMedia, Mumbai (India). Fetal bovine serum used for cell culture media was procured from Invitrogen. Phosphohistone H3 (Ser-10) primary antibody was purchased from Santa Cruz Biotech. All the reagents utilized for the experiments were of analytical grade.

Cell Culture. MCF-7, HeLa and MDA-MB-231 were purchased from the cell repository of National Centre for Cell Science, Pune, India. EMT6/AR1 cell line was purchased from Sigma, and HuH-7 cells were obtained from the laboratory of Dr. S. Das (Indian Institute of Science, Bangalore, India). HeLa and MCF-7 cells were cultured in minimal essential media (MEM), whereas MDA-MB-231, HuH-7, and EMT6AR1 was cultured in Dulbecco's Modified Eagle'S Medium supplemented with 2.2 g/L of sodium bicarbonate, 10% (v/v) fetal bovine serum (FBS: US origin), and 1% antibiotic−antimycotic solution composed of streptomycin, amphotericin B, and penicillin. Cell lines were cultured at 37 °C in a humidified incubator (Sanyo, Tokyo, Japan) with 5% carbon dioxide.

Cell-Based Screening Assay. Synthesized combretastatin analogues, (**1**−**15**) and CA-4 used in the study were dissolved in 100% cell culture grade DMSO. The compounds were serially diluted in minimal essential media (MEM) to maintain the final concentration of DMSO as <0.1% for testing on cancer cell lines. A concentration of 200 nM of synthesized combretastatin analogues (**1**−**15**) and CA-4 were initially used for screening the potency of compounds in HeLa cell line.

Half-Maximal Inhibition of Tumor Cell Growth by Combretastatin Analogues. MCF-7 and HeLa cells (1 × 10^5 cells/mL) were seeded in 96-well plates and incubated for 24 h for attachment. The cells were then incubated with different concentrations of synthesized combretastatin analogues and incubated for 48 h for MCF-7 and 24 h for HeLa. CA-4 was used as a control for comparing the potencies of the synthesized combretastatin analogues. MDA-MB-231, EMT6AR1, and HuH-7 cells were incubated with compound **12** and CA-4 for 24 h. Subsequently, cells were fixed with 50% TCA and the half-maximal inhibitory concentration (IC_{50}) for the respective compounds was determined by sulforhodamine B assay.[58] Three independent sets of experiments were performed.

Immunostaining and Microscopy. MCF-7 cells (0.5 × 10^5 cells/mL) were seeded on glass coverslips in a 24-well tissue culture plate for 24 h and then incubated without or with different concentrations of compound **12** for 24 h. The cells were fixed with 3.7% formaldehyde and stained with α-tubulin (IgG) or phosphohistone H3 (Ser-10) antibodies for 1 h. Then, FITC conjugated IgG secondary antibody were added onto the cells and incubated for 1 h and washed with DPBS three times. The cells were finally stained with (20 μg/mL) of Hoechst 33258. The images were captured using an Eclipse TE 2000U microscope (Nikon, Tokyo, Japan).

DOI: 10.1021/acs.jmedchem.6b00101
J. Med. Chem. XXXX, XXX, XXX−XXX

Cell Migration Assay. MDA-MB-231 cells were grown in 35 mm culture dishes until 90% confluency. Subsequently, the media was aspirated and a wound was created in the middle of the dish by scratching on the confluent cells using a 10 μL microtip.[59] The cells were then incubated in the absence and presence of different concentrations of compound **12** and CA-4. The wound closure was monitored at different time points (0, 4, and 18 h). Images were captured and the percentage of wound closure was calculated using Image Pro-Plus software.

Cell Cycle Analysis by Flow Cytometry. MCF-7 cells were incubated in the absence and presence of compound **12** and CA-4 for 24 h. Subsequently, the cells were fixed with 70% alcohol in DPBS. The fixed cells were incubated with RNase (1 μg/mL) and propidium iodide (50 μg/mL) for 2 h. The flow cytometry analysis were performed using BD FACS Aria special order system (Becton Dickinson, San Jose, CA, USA), and the obtained data were fitted using a software, Modfit LT version 3.2 (Verity Software House, ME, USA).[60]

*The Effects of Compounds **12**, **9**, and **6** on the Assembly Kinetics of Tubulin in Vitro.* Tubulin was purified from goat brains using 1 M glutamate as described previously.[61] The purity of tubulin was estimated to be >97% using Coomassie Brilliant Blue stained SDS-PAGE. Tubulin (12 μM) was resuspended in a buffer containing 25 mM PIPES, 1 mM EGTA, and 3 mM $MgCl_2$ with 1 M glutamate and was incubated without or with different concentrations (0.5−5 μM) of compound **12**, (0.5 to 20 μM) of compound **9**, (5−40 μM) of compound **6**, and (0.5−5 μM) of CA-4 for 10 min on ice. After 10 min, 1 mM GTP was added to the reaction mixtures, and subsequently, the assembly kinetics of tubulin was monitored at 350 nm (37 °C) for 20 min using Spectramax M2^e. Similarly, inhibition of the assembly kinetics of tubulin was tested using CA4 for comparison of the potency of compound **12**. Three independent experiments were performed.

*Determination of the Dissociation Constant (K_d) of the Binding of Compound **12** and Tubulin.* Tubulin (2 μM) was incubated in the absence and presence of different concentrations (1−20 μM) of compound **12** for 10 min at 25 °C. Tryptophan fluorescence of tubulin in the presence and absence of compound **12** was monitored using an excitation wavelength of 295 nm in a 0.3 cm path length cuvette (FP-6500 spectrofluorometer JASCO, Tokyo, Japan). A dissociation constant for the binding interaction of compound **12** and tubulin was calculated by fitting the change in fluorescence data in an equation $\Delta F = \frac{\Delta F\max \times L}{K_d + L}$ using Graph Pad Prism software version 5. Four independent sets of experiments were performed.

*Characterization of the Binding of Compound **12** on Tubulin.* Tubulin (2 μM) was incubated without and with different concentrations of compound **12** (5 and 10 μM) in 25 mM PIPES buffer, pH 6.8, for 10 min at 25 °C. The fluorescence spectra (420−520 nm) were recorded using an excitation wavelength of 350 nm. The experiments were repeated thrice.

*Determination of the Binding Site of Compound **12** on Tubulin.* Tubulin (3 μM) was incubated without or with different concentrations (1−20 μM) of podophyllotoxin in 25 mM PIPES, pH 6.8, for 15 min at 25 °C. Subsequently, compound **12** (6 μM) was added to all the reaction mixtures and incubated for 15 min at 25 °C. Similar experiments were performed using tubulin (3 μM) with different concentrations of (1−20 μM) of CA-4, vinblastine (10 and 30 μM), and paclitaxel (10 and 30 μM) in 25 mM PIPES, pH 6.8, for 15 min at 25 °C. Subsequently, the reaction mixtures were incubated with 6 μM compound **12** for 15 min at 25 °C. After the incubation, the fluorescence spectra (420−520 nm) were recorded using an excitation wavelength of 350 nm. The inhibition constant was calculated using an equation.

$$K_i = \frac{EC_{50}}{1 + \frac{L}{K_d}}$$

In a separate experiment, tubulin was first incubated with compound **12** for 30 min. Then the reaction mixture was incubated without or with either 50 μM podophyllotoxin or 50 μM CA-4 for an additional 30 min. The spectra were monitored using 350 nm as the excitation wavelength.

■ ASSOCIATED CONTENT

Supporting Information

The Supporting Information is available free of charge on the ACS Publications website at DOI: 10.1021/acs.jmedchem.6b00101.

Spectral data of intermediates and compounds **1**−**15**, scanned copies of ^{1}H NMR and ^{13}C NMR of intermediates and **1**−**15**, reversible binding of compound **12** to tubulin, and effects of vinblastine and paclitaxel on the binding of **12** to tubulin (PDF)

Molecular formula strings (CSV)

■ AUTHOR INFORMATION

Corresponding Authors

*For S.K.G.: phone, +91 (0)172 2214683; fax, +91 (0) 1722214692; E-mail, skguchhait@niper.ac.in, skguchhait@gmail.com.

*For D.P.: phone, +91 222 576 7838; fax, +91 222 572 3480; E-mail, panda@iitb.ac.in.

Author Contributions

‖V.C. and J.B.V. contributed equally to this work.

Notes

The authors declare no competing financial interest.

■ ACKNOWLEDGMENTS

We gratefully acknowledge the financial support from DAE-SRC, DST, and CSIR, Government of India, for this investigation. D.P. thanks DAE-SRC fellowship. V.C. is thankful to CSIR, Government of India for his fellowship. A.S.B. is thankful to NIPER for his fellowship.

■ ABBREVIATIONS USED

NBS, *N*-bromosuccinimide; EtOAc, ethyl acetate; KOAc, potassium acetate; $Pd(OAc)_2$, palladium acetate; DMAc, dimethylacetamide; $Cu(Ac)_2$, copper(II) acetate; TBAB, tetrabutylammonium bromide; $Pd(PPh_3)_4$, tetrakis-(triphenylphosphine)palladium(0); Pd/C, palladium on carbon; MeOH, methanol; DMSO, dimethyl sulfoxide; PIPES, piperazine-*N*,*N*′-bis(ethanesulfonic acid); EGTA, ethylene glycol-bis(2-aminoethyl ether)-*N*,*N*,*N*′,*N*′-tetraacetic acid; GTP, guanosine-5′-triphosphate; DPBS, Dulbecco's phosphate buffered saline; TLC, thin layer chromatography:

■ REFERENCES

(1) Jordan, M. A.; Wilson, L. Microtubules as a target for anticancer drugs. *Nat. Rev. Cancer* **2004**, *4*, 253−265.

(2) Li, Q.; Sham, H. L. Discovery and development of antimitotic agents that inhibit tubulin polymerisation for the treatment of cancer. *Expert Opin. Ther. Pat.* **2002**, *12*, 1663−1702.

(3) Mukhtar, E.; Adhami, V. M.; Mukhtar, H. Targeting microtubules by natural agents for cancer therapy. *Mol. Cancer Ther.* **2014**, *13*, 275−284.

(4) Nogales, E.; Whittaker, M.; Milligan, R. A.; Downing, K. H. High-Resolution model of the microtubule. *Cell* **1999**, *96*, 79−88.

(5) Ravelli, R. B.; Gigant, B.; Curmi, P. A.; Jourdain, I.; Lachkar, S.; Sobel, A.; Knossow, M. Insight into tubulin regulation from a complex with colchicine and a stathmin-like domain. *Nature* **2004**, *428*, 198−202.

(6) Nam, N. H. Combretastatin A-4 analogues as antimitotic antitumor agents. *Curr. Med. Chem.* **2003**, *10*, 1697−1722.

DOI: 10.1021/acs.jmedchem.6b00101
J. Med. Chem. XXXX, XXX, XXX−XXX

(7) Bohlin, L.; Rosen, B. Podophyllotoxin derivatives: drug discovery and development. *Drug Discovery Today* **1996**, *1*, 343−351.
(8) Kupchan, S. M.; Britton, R. W.; Ziegler, M. F.; Gilmore, C. J.; Restivo, R. J.; Bryan, R. F. Steganacin and steganangin, novel antileukemic lignan lactones from Steganotaenia araliacea. *J. Am. Chem. Soc.* **1973**, *95*, 1335−1336.
(9) (a) Jordan, A.; Hadfield, J. A.; Lawrence, N. J.; McGown, A. T. Tubulin as a target for anticancer drugs: agents which interact with mitotic spindle. *Med. Res. Rev.* **1998**, *18*, 259−296. (b) Alvarez, C.; Alvarez, R.; Corchete, P.; Pérez-Melero, C.; Peláez, R.; Medarde, M. Exploring the effect of 2,3,4-trimethoxy-phenyl moiety as a component of indolephenstatins. *Eur. J. Med. Chem.* **2010**, *45*, 588−597. (c) Brancale, A.; Silvestri, R. Indole, a core nucleus for potent inhibitors of tubulin polymerization. *Med. Res. Rev.* **2007**, *27*, 209−238. (d) Ray, K.; Bhattacharyya, B.; Biswas, B. B. Role of B-ring of colchicine in its binding to tubulin. *J. Biol. Chem.* **1981**, *256*, 6241−6244.
(10) Pettit, G. R.; Singh, S. B.; Hamel, E.; Lin, C. M.; Alberts, D. S.; Garcia-Kendal, D. Isolation and structure of the strong cell growth and tubulin inhibitor combretastatin A-4. *Experientia* **1989**, *45*, 209−211.
(11) (a) Hamel, E. Antimitotic natural products and their interactions with tubulin. *Med. Res. Rev.* **1996**, *16*, 207−231. (b) Jordan, M. A.; Wilson, L. Microtubules as a target for anticancer drugs. *Nat. Rev. Cancer* **2004**, *4*, 253−265. (c) Woods, J. A.; Hadfield, J. A.; Pettit, G. R.; Fox, B. W.; McGown, A. T. The interaction with tubulin of a series of stilbenes based on combretastatin A-4. *Br. J. Cancer* **1995**, *71*, 705−711.
(12) Lin, C. M.; Ho, H. H.; Pettit, G. R.; Hamel, E. Antimitotic natural products combretastatin A-4 and combretastatin A-2: studies on the mechanism of their inhibition of the binding of colchicine to tubulin. *Biochemistry* **1989**, *28*, 6984−6991.
(13) Patterson, D. M.; Rustin, G. J. S. Vascular damaging agents. *Clin. Oncol.* **2007**, *19*, 443−456.
(14) Nagaiah, G.; Remick, S. C. CA-4 phosphate: a novel vascular disrupting agent. *Future Oncol.* **2010**, *6*, 1219−1228.
(15) (a) Dowlati, A.; Robertson, K.; Cooney, M.; Petros, W. P.; Stratford, M.; Jesberger, J.; Rafie, N.; Overmoyer, B.; Makkar, V.; Stambler, B.; Taylor, A.; Waas, J.; Lewin, J. S.; McCrae, K. R.; Remick, S. C. A phase I pharmacokinetic and translational study of the novel vascular targeting agent combretastatin A-4 phosphate on a single-dose intravenous schedule in patients with advanced cancer. *Cancer Res.* **2002**, *62*, 3408−3416. (b) Rustin, G. J.; Galbraith, S. M.; Anderson, H.; Stratford, M.; Folkes, L. K.; Sena, L.; Gumbrell, L.; Price, P. M. Phase I clinical trial of weekly CA-4 phosphate: clinical and pharmacokinetic results. *J. Clin. Oncol.* **2003**, *21*, 2815−2822.
(16) Hori, K.; Saito, S. Microvascular mechanisms by which the combretastatin A-4 derivative AC7700 (AVE8062) induces tumour blood flow stasis. *Br. J. Cancer* **2003**, *89*, 1334−1344.
(17) Hua, J.; Sheng, Y.; Pinney, K. G.; Garner, C. M.; Kane, R. R.; Prezioso, J. A.; Pettit, G. R.; Chaplin, D. J.; Edvardsen, K. Oxi4503, a novel vascular targeting agent: effects on blood flow and antitumor activity in comparison to combretastatin A-4 phosphate. *Anticancer Res.* **2003**, *23*, 1433−1440.
(18) Wang, L.; Woods, K. W.; Li, Q.; Barr, K. J.; McCroskey, R. W.; Hannick, S. M.; Gherke, L.; Credo, R. B.; Hui, Y.-H.; Marsh, K.; Warner, R.; Lee, J. Y.; Zielinski-Mozng, N.; Frost, D.; Rosenberg, S. H.; Sham, H. L. Potent, orally active heterocycle-based combretastatin A-4 analogues: synthesis, structure-activity relationship, pharmacokinetics, and in vivo antitumor activity evaluation. *J. Med. Chem.* **2002**, *45*, 1697−1711.
(19) Tron, G. C.; Pirali, T.; Sorba, G.; Pagliai, F.; Busacca, S.; Genazzani, A. A. Medicinal chemistry of CA-4: present and future directions. *J. Med. Chem.* **2006**, *49*, 3033−3044.
(20) Aprile, S.; Del Grosso, E.; Tron, G. C.; Grosa, G. In vitro metabolism study of combretastatin A-4 in rat and human liver microsomes. *Drug Metab. Dispos.* **2007**, *35*, 2252−2261.
(21) Kim, Y.; Nam, N.-H.; You, Y.-J.; Ahn, B.-Z. Synthesis and cytotoxicity of 3,4-diaryl-2(5H)-furanones. *Bioorg. Med. Chem. Lett.* **2002**, *12*, 719−722.
(22) Nam, N.-H.; Kim, Y.; You, Y.-J.; Hong, D.-H.; Kim, H.-M.; Ahn, B.-Z. Combretoxazolones: synthesis, cytotoxicity and antitumor activity. *Bioorg. Med. Chem. Lett.* **2001**, *11*, 3073−3076.
(23) Bailly, C.; Bal, C.; Barbier, P.; Combes, S.; Finet, J. − P.; Hildebrand, M. − P.; Peyrot, V.; Wattez, N. Synthesis and biological evaluation of 4-arylcoumarin analogues of combretastatins. *J. Med. Chem.* **2003**, *46*, 5437−5444.
(24) Tron, G. C.; Pagliai, F.; Del Grosso, E.; Genazzani, A. A.; Sorba, G. Synthesis and cytotoxic evaluation of combretafurazans. *J. Med. Chem.* **2005**, *48*, 3260−3268.
(25) Pati, H. N.; Wicks, M.; Holt, H. L., Jr.; LeBlanc, R.; Weisbruch, P.; Forrest, L.; Lee, M. Synthesis and biological evaluation of cis-combretastatin analogs and their novel 1,2,3-triazole derivatives. *Heterocycl. Commun.* **2005**, *11*, 117−120.
(26) Simoni, D.; Grisolia, G.; Giannini, G.; Roberti, M.; Rondanin, R.; Piccagli, L.; Baruchello, R.; Rossi, M.; Romagnoli, R.; Invidiata, F. P.; Grimaudo, S.; Jung, M. K.; Hamel, E.; Gebbia, N.; Crosta, L.; Abbadessa, V.; Di Cristina, A.; Dusonchet, L.; Meli, M.; Tolomeo, M. Heterocyclic and phenyl double-bond-locked combretastatin analogues possessing potent apoptosis-inducing activity in HL60 and in MDR cell lines. *J. Med. Chem.* **2005**, *48*, 723−736.
(27) Romagnoli, R.; Baraldi, P. G.; Brancale, A.; Ricci, A.; Hamel, E.; Bortolozzi, R.; Basso, G.; Viola, G. Convergent synthesis and biological evaluation of 2-amino-4- (3′,4′,5′-trimethoxyphenyl)-5-aryl thiazoles as microtubule targetingagents. *J. Med. Chem.* **2011**, *54*, 5144−5153.
(28) Beale, T. M.; Allwood, D. M.; Bender, A.; Bond, P. J.; Brenton, J. D.; Charnock-Jones, D. S.; Ley, S. V.; Myers, R. M.; Shearman, J. W.; Temple, J.; Unger, J.; Watts, C. A.; Xian, J. A-ring dihalogenation increases the cellular activity of combretastatin-templated tetrazoles. *ACS Med. Chem. Lett.* **2012**, *3*, 177−181.
(29) La Regina, G.; Bai, R.; Coluccia, A.; Famiglini, V.; Pelliccia, S.; Passacantilli, S.; Mazzoccoli, C.; Ruggieri, V.; Verrico, A.; Miele, A.; Monti, L.; Nalli, M.; Alfonsi, R.; Di Marcotullio, L.; Gulino, A.; Ricci, B.; Soriani, A.; Santoni, A.; Caraglia, M.; Porto, S.; Da Pozzo, E.; Martini, C.; Brancale, A.; Marinelli, L.; Novellino, E.; Vultaggio, S.; Varasi, M.; Mercurio, C.; Bigogno, C.; Dondio, G.; Hamel, E.; Lavia, P.; Silvestri, R. New indole tubulin assembly inhibitors cause stable arrest of mitotic progression, enhanced stimulation of natural killer cell cytotoxic activity and repression of Hedgehog-dependent cancer. *J. Med. Chem.* **2015**, *58*, 5789−5807.
(30) (a) Chen, H.; Li, Y.; Sheng, C.; Lv, Z.; Dong, G.; Wang, T.; Liu, J.; Zhang, M.; Li, L.; Zhang, T.; Geng, D.; Niu, C.; Li, K. Design and synthesis of cyclopropylamide analogues of combretastatin-A4 as novel microtubule-stabilizing agents. *J. Med. Chem.* **2013**, *56*, 685−699. (b) Jonnalagadda, S. S.; ter Haar, E.; Hamel, E.; Lin, C. M.; Magarian, R. A.; Day, B. W. Synthesis and biological evaluation of 1,1-dichloro-2,3-diarylcyclopropanes as antitubulin and anti-breast cancer agents. *Bioorg. Med. Chem.* **1997**, *5*, 715−722.
(31) Nam, N. − H.; Kim, Y.; You, Y. − J.; Hong, D. − H.; Kim, H. − M.; Ahn, B. − Z. Synthesis and anti-tumor activity of novel combretastatins: combretocyclopentenones and related analogues. *Bioorg. Med. Chem. Lett.* **2002**, *12*, 1955−1958.
(32) (a) Nien, C.-Y.; Chen, Y.-C.; Kuo, C.-C.; Hsieh, H.-P.; Chang, C.-Y.; Wu, J.-S.; Wu, S.-Y.; Liou, J.-P.; Chang, J.-Y. 5-Amino-2-aroylquinolines as highly potent tubulin polymerization inhibitors. *J. Med. Chem.* **2010**, *53*, 2309−2313. (b) Pettit, G. R.; Toki, B.; Herald, D. L.; Verdier-Pinard, P.; Boyd, M. R.; Hamel, E.; Pettit, R. K. Antineoplastic agents. 379. Synthesis of phenstatin phosphate. *J. Med. Chem.* **1998**, *41*, 1688−1695. (c) Liou, J. P.; Chang, C. W.; Song, J. W.; Yang, Y. N.; Yeh, C. F.; Tseng, H. Y.; Lo, Y. K.; Chang, Y. L.; Chang, C. M.; Hsieh, H. P. Synthesis and struture-reactivity relationship of 2-aminobenzophenone derivatives as antimitotic agents. *J. Med. Chem.* **2002**, *45*, 2556−2562.
(33) La Regina, G.; Edler, M. C.; Brancale, A.; Kandil, S.; Coluccia, A.; Piscitelli, F.; Hamel, E.; De Martino, G. D.; Matesanz, R.; Díaz, J. F.; Scovassi, A. I.; Prosperi, E.; Lavecchia, A.; Novellino, E.; Artico, M.; Silvestri, R. Arylthioindole inhibitors of tubulin polymerization. 3. Biological evaluation, structure-activity relationships and molecular modeling studies. *J. Med. Chem.* **2007**, *50*, 2865−2874.

DOI: 10.1021/acs.jmedchem.6b00101
J. Med. Chem. XXXX, XXX, XXX−XXX

(34) Lawrence, N. J.; Rennison, D.; Woo, M.; McGown, A. T.; Hadfield, J. A. Antimitotic and cell growth inhibitory properties of combretastatin A-4-like ethers. *Bioorg. Med. Chem. Lett.* **2001**, *11*, 51−54.
(35) Ohsumi, K.; Nakagawa, R.; Fukuda, Y.; Hatanaka, T.; Morinaga, Y.; Nihei, Y.; Ohishi, K.; Suga, Y.; Akiyama, Y.; Tsuji, T. Novel combretastatin analogues effective against murine solid tumors: Design and structure-activity relationships. *J. Med. Chem.* **1998**, *41*, 3022−3032.
(36) (a) Gwaltney, S. L., II; Imade, H. M.; Barr, K. J.; Li, Q.; Gehrke, L.; Credo, R. B.; Warner, R. B.; Lee, J. Y.; Kovar, P.; Wang, J.; Nukkala, M. A.; Zielinski, N. A.; Frost, D.; Ng, S.-C.; Sham, H. L. Novel sulfonate analogues of combretastatin A-4: potent antimitotic agents. *Bioorg. Med. Chem. Lett.* **2001**, *11*, 871−874. (b) Lee, H.-Y.; Chang, J.-Y.; Nien, C.-Y.; Kuo, C.-C.; Shih, K.-H.; Wu, C.-H.; Chang, C.-Y.; Lai, W.-Y.; Liou, J.-P. 5-Amino-2-aroylquinolines as highly potent tubulin polymerization inhibitors. part 2. The impact of bridging groups at position C-2. *J. Med. Chem.* **2011**, *54*, 8517−8525.
(37) Kandekar, S.; Preet, R.; Kashyap, M.; M U, R. P.; Mohapatra, P.; Das, D.; Satapathy, S. R.; Siddharth, S.; Jain, V.; Choudhuri, M.; Kundu, C. N.; Guchhait, S. K.; Bharatam, P. V. Structural elaboration of a natural product: identification of 3,3′-diindolylmethane amino-phosphonate and urea derivatives as potent anticancer agents. *ChemMedChem* **2013**, *8*, 1873−1884.
(38) Sanghai, N.; Jain, V.; Preet, R.; Kandekar, S.; Das, S.; Trivedi, N.; Mohapatra, P.; Priyadarshani, G.; Kashyap, M.; Das, D.; Satapathy, S. R.; Siddharth, S.; Guchhait, S. K.; Kundu, C. N.; Bharatam, P. V. Combretastatin A-4 inspired novel 2-aryl-3-arylamino-imidazo-pyridines/pyrazines as tubulin polymerization inhibitors, antimitotic and anticancer agents. *Med. Chem. Commun.* **2014**, *5*, 766−782.
(39) Al-Mourabit, A.; Zancanella, M. A.; Tilvi, S.; Romo, D. Biosynthesis, asymmetric synthesis, and pharmacology, including cellular targets, of the pyrrole-2-aminoimidazole marine alkaloids. *Nat. Prod. Rep.* **2011**, *28*, 1229−1260.
(40) Zidar, N.; Montalvão, S.; Hodnik, Ž.; Nawrot, D. A.; Žula, A.; Ilaš, J.; Kikelj, D.; Tammela, P.; Mašič, L. P. Antimicrobial activity of the marine alkaloids, clathrodin and oroidin, and their synthetic analogues. *Mar. Drugs* **2014**, *12*, 940−963.
(41) Keifer, P. A.; Schwartz, R. E.; Koker, M. E. S.; Hughes, J. R. G.; Rittschof, D.; Rinehart, K. L. Bioactive bromopyrrole metabolites from the caribbean sponge Agelas conifera. *J. Org. Chem.* **1991**, *56*, 2965−2975.
(42) Walker, R. P.; Faulkner, D. J.; Van Engen, D. V.; Clardy, J. Sceptrin, an antimicrobial agent from the sponge Agelas sceptrum. *J. Am. Chem. Soc.* **1981**, *103*, 6772−6773.
(43) Kobayashi, J.; Tsuda, M.; Murayama, T.; Nakamura, H.; Ohizumi, Y.; Ishibashi, M.; Iwamura, M.; Ohta, T.; Nozoe, S. Ageliferins, potent actomyosin Atpase activators from the Okinawan marine sponge. *Tetrahedron* **1990**, *46*, 5579−5586.
(44) Huigens, R. W., III; Richards, J. J.; Parise, G.; Ballard, T. E.; Zeng, W.; Deora, R.; Melander, C. Inhibition of pseudomonas aeruginosa biofilm formation with bromoageliferin analogues. *J. Am. Chem. Soc.* **2007**, *129*, 6966−6967.
(45) Nishimura, T.; Kitajima, K. Reaction of guanidines with a-diketones. Syntheses of 4,5-disubstituted-2- aminoimidazoles and 2,6-unsymmetrically substituted imidazo[4,5-*d*]imidazoles. *J. Org. Chem.* **1979**, *44*, 818−824.
(46) Bhaskar, V. H.; Sarath, K.; Kumar, M. Synthesis and antiinflammatory activity of some 2-(substituted phenyl)-3-(4,5-diphenyl-1*H*-imidazol-2-yl)-1,3-thiazolidin-4-one. *Asian J. Chem.* **2008**, *20*, 5133−5138.
(47) (a) Soh, C. H.; Chui, W. K.; Lam, Y. An efficient and expeditious synthesis of di- and monosubstituted 2-aminoimidazoles. *J. Comb. Chem.* **2008**, *10*, 118−122. (b) Little, T. L.; Webber, S. E. A simple and practical synthesis of 2-aminoimidazoles. *J. Org. Chem.* **1994**, *59*, 7299−7305.
(48) Worthington, R. J.; Bunders, C. A.; Reed, C. S.; Melander, C. Small molecule suppression of carbapenem resistance in NDM-1 producing klebsiella pneumonia. *ACS Med. Chem. Lett.* **2012**, *3*, 357−361.
(49) Ermolat'ev, D. S.; Svidritsky, E. P.; Babaev, E. V.; Van der Eycken, E. Microwave-assisted synthesis of substituted 2-amino-1*H*-imidazoles from imidazo[1,2- *a*]pyrimidines. *Tetrahedron Lett.* **2009**, *50*, 5218−5220.
(50) Santra, A.; Bagdi, A. K.; Majee, A.; Hajra, A. Iron(III)-catalyzed cascade reaction between nitroolefines and 2-aminopyridines: Synthesis of imidazo [1,2-*a*] pyridines and easy access towards zolimidine. *Adv. Synth. Catal.* **2013**, *355*, 1065−1070.
(51) Song, G.; Zhang, Y.; Li, X. Rhodium and Iridium complexes of abnormal N-heterocyclic carbenes derived from Imidazo[1,2-*a*]-pyridine. *Organometallics* **2008**, *27*, 1936−1943.
(52) Bagdi, A. K.; Rahman, M.; Santra, S.; Majee, A.; Hajra, A. Copper-catalyzed synthesis of imidazo [1,2-*a*]pyridines through tandem imine formation-oxidative cyclization under ambient air: One-step synthesis of zolimidine on a gram-scale. *Adv. Synth. Catal.* **2013**, *355*, 1741−1747.
(53) Fu, H. Y.; Chen, L.; Doucet, H. Phosphine-free palladium-catalyzed direct arylation of imidazo [1,2-*a*] pyridines with aryl bromides at low catalyst loading. *J. Org. Chem.* **2012**, *77*, 4473−4478.
(54) Wang, H.; Ma, Y.; Tian, H.; Yu, A.; Chang, J.; Wu, Y. Tetrabutyl ammonium bromide-mediated benzylation of phenols in water under mild condition. *Tetrahedron* **2014**, *70*, 2669−2673.
(55) Ermolat'ev, D. S.; Giménez, V. N.; Babaev, E. V.; Van der Eycken, E. Efficient Pd(0)-mediated microwave-assisted arylation of 2-substituted imidazo[1,2-*a*]pyrimidines. *J. Comb. Chem.* **2006**, *8*, 659−663.
(56) Cortese, F.; Bhattacharyya, B.; Wolff, J. Podophyllotoxin as a probe for the colchicine binding site of tubulin. *J. Biol. Chem.* **1977**, *252*, 1134−1140.
(57) Sackett, D. L. Podophyllotoxin, steganacin and combretastatin: natural products that bind at the colchicine site of tubulin. *Pharmacol. Ther.* **1993**, *59*, 163−228.
(58) Skehan, P.; Storeng, R.; Scudiero, D.; Monks, A.; McMahon, J.; Vistica, D.; Warren, J. T.; Bokesch, H.; Kenney, S.; Boyd, M. R. New colorimetric cytotoxicity assay for anticancer-drug screening. *J. Natl. Cancer. Inst.* **1990**, *82*, 1107−1112.
(59) Kapoor, S.; Panda, D. Kinetic stabilization of microtubule dynamics by indanocine perturbs EB1 localization, induces defects in cell polarity and inhibits migration of MDA-MB-231 cells. *Biochem. Pharmacol.* **2012**, *83*, 1495−1506.
(60) Venghateri, J. B.; Gupta, T. K.; Verma, P. J.; Kunwar, A.; Panda, D. Ansamitocin P3 depolymerizes microtubules and induces apoptosis by binding to tubulin at the vinblastine site. *PLoS One* **2013**, *8*, e75182.
(61) Hamel, E.; Lin, C. M. Glutamate-induced polymerization of tubulin: characteristics of the reaction and application to the large-scale purification of tubulin. *Arch. Biochem. Biophys.* **1981**, *209*, 29−40.

DOI: 10.1021/acs.jmedchem.6b00101
J. Med. Chem. XXXX, XXX, XXX−XXX